Compressibility effect on magnetic-shear-localized ideal magnetohydrodynamic interchange instability

Sangeeta Gupta, J. D. Callen, and C. C. Hegna
Department of Engineering Physics, University of Wisconsin, Madison, Wisconsin 53706-1609

(Received 28 February 2005; accepted 15 June 2005; published online 25 July 2005)

Eigenmode analysis of a magnetic-shear-localized ideal magnetohydrodynamic interchange instability in the presence of plasma compressibility indicates the marginal stability criterion ($D_I = 1/4$) is not affected by the compressibility effects. Above the marginal stability criterion, plasma compressibility causes a significant reduction in the growth rate of an ideal interchange instability. © *2005 American Institute of Physics*. [DOI: 10.1063/1.1992987]

I. INTRODUCTION

The Suydam criterion[1,2] defines the stability condition for a localized ideal magnetohydrodynamics (MHD) interchange mode in an incompressible cylindrical plasma. It is given by

$$D_I \leqslant 1/4, \quad \text{for stability}. \tag{1}$$

Here, the driving term for instability is $D_I \equiv -(8\pi p_0'/B_z^2 r_s) \times (q/q')^2 \equiv \beta L_s^2/r_p R_c$ in which $1/L_s \equiv (1/R_0 q)(rq'/q), \beta/r_p \equiv -8\pi P_0'/B_z^2$ and R_c is the average magnetic field curvature radius. In a toroidal geometry, the stability regime (known as the Mercier criterion) is again $D_I \leqslant 1/4$ for stability.[1,3] For an axisymmetric tokamak in the limit of large aspect ratio, small β and circular cross-section, the form of D_I in the Mercier criterion is $D_I = -(8\pi p_0'/B_\phi^2 r)(q/q')^2(1-q^2)$.[1,4] In these derivations, the mode is assumed to be localized arbitrarily close to the mode rational surface.

The Mercier (Suydam) criterion is expected to define an operational limit for toroidal devices. However, there is no definitive experimental evidence to support this thesis. In particular, a number of experiments on high-β stellarator configurations have shown no discernable degradation in the plasma operation when operating in a Mercier unstable region ($D_I > 1/4$).[5–9] The physics of what controls the β limit in currentless stellarator operation is a topic of considerable interest. Understanding why Mercier stability predictions do not limit operation is a primary motivation for the work presented here.

Linear eigenmode analysis of the magnetic-shear-localized ideal MHD interchange instability indicates that the growth rate is exponentially small for D_I values just above the critical value of 1/4.[10–12] The criterion for "robust" growth appears to be almost a factor of 2 greater than the Suydam criterion. In the presence of plasma electrical resistivity, resistive-g or resistive interchange modes become unstable for $D_I > 0$[13–15] with reduced growth rate. The usual nonideal effects such as finite ion Larmor radius, electron diamagnetic flow and resistivity do not alter the higher criterion for robust growth.[12] Another possible effect that can alter the growth rate of magnetic-shear-localized ideal interchange instabilities is the effect of compressibility, i.e., the effect of coupling to sound waves. From the pressure evolution equation, it is clear that the compressibility effects become important only when $\omega^2 \gtrsim k_\parallel^2 C_s^2$ where $k_\parallel = k_y x/L_s$ in the sheared slab model and $C_s \equiv \sqrt{\Gamma_0 P_0/\rho_{m0}}$. Thus, close to the mode rational surface (i.e., near $x=0$), this condition can be satisfied easily for any arbitrary ω. In this paper, we explore the effect of compressibility on the linear stability properties of the magnetic-shear-localized ideal MHD interchange instabilities in a sheared slab model. Our analytical analysis shows that the marginal stability condition (i.e., $D_I = 1/4$) is unaffected by the compressional effects, consistent with δW analysis. For $D_I > 1/4$, compressibility has a stabilizing effect that can significantly affect the instability growth rate.

The paper is organized a follows. Section II describes the basic model used for studying the compressible interchange instability. In Sec. III, the linear eigenvalue equation is solved analytically using a matched asymptotic analysis. Finally, conclusions are presented in Sec. IV.

II. BASIC MODEL

We consider a sheared slab model where the magnetic field is represented locally by

$$\vec{B} = B_0 \left[\left(1 + \frac{x}{L_B}\right)\hat{e}_z + \frac{z}{R_c}\hat{e}_x + \frac{x}{L_s}\hat{e}_y \right]. \tag{2}$$

Here $\hat{e}_x$, $\hat{e}_y$ and $\hat{e}_z$ are unit vectors along x, y and $z, L_B = (d \ln B/dx)^{-1}$ is the scale length of the perpendicular gradient of magnetic field strength, $L_s = B(dB_y/dx)^{-1}$ is the magnetic shear scale length and $\kappa = -1/R_c$ is the curvature of the magnetic field. Here, $R_c > 0$ represents good curvature and $R_c < 0$ represents bad curvature. In equilibrium, the radial force balance equation gives $d(P_0 + B^2/8\pi)/dx = B_0 B_z/4\pi R_c$, implying $\beta/r_p = 1/R_c - 1/L_B$. On the other hand, in the direction parallel to the equilibrium magnetic field, pressure is constant, i.e., $\nabla_\parallel P_0 = 0$.

To derive an eigenvalue equation for ideal interchange instabilities, we consider a low β plasma (i.e., $\beta \equiv 8\pi P_0/B^2 \ll 1$), which allows us to neglect the compressional component of magnetic field perturbations. Thus, we can write $\vec{E}_\perp = -\vec{\nabla}_\perp \phi_1$ and $E_\parallel = -\nabla_\parallel \phi_1 - (1/c)\partial A_\parallel/\partial t$ where ϕ_1 is the scalar potential perturbations and $A_\parallel [\equiv (\vec{A}_1 \cdot \vec{B})/|B|]$ is the parallel vector potential perturbation.

Thus, the linearized equations describing the magnetic-shear-localized ideal interchange mode for a compressible plasma are:[16,17]

$$\rho_m \frac{c^2}{B^2}\frac{d}{dt}\nabla_\perp^2\tilde{\phi} + \frac{2c}{B^2}\vec{B}\times\vec{\nabla}\tilde{p}\cdot\vec{\kappa} - (\vec{B}\cdot\vec{\nabla})\left(\frac{\tilde{J}_\parallel}{B}\right) = 0, \quad (3)$$

$$\vec{\tilde{V}}_\perp = \frac{c}{B^2}\vec{B}\times\vec{\nabla}\tilde{\phi}, \quad \frac{1}{c}\frac{\partial\tilde{\psi}}{\partial t} = -\nabla_\parallel\tilde{\phi}, \quad (4)$$

$$\tilde{J}_\parallel = -\frac{c}{4\pi}\nabla_\perp^2\tilde{\psi}, \quad \frac{\partial\tilde{p}}{\partial t} = -\tilde{V}\cdot\vec{\nabla}P_0 - \Gamma_0 P_0\vec{\nabla}\cdot\vec{\tilde{V}}, \quad (5)$$

$$\rho_m\frac{\partial\tilde{V}_\parallel}{\partial t} = -\nabla_\parallel\tilde{p} + \frac{1}{B^2}\vec{B}\times\vec{\nabla}\tilde{\psi}\cdot\vec{\nabla}P_0, \quad (6)$$

where $\tilde{J}_\parallel \equiv (\vec{B}\cdot\vec{\tilde{J}})/|B|$ is the parallel component of the current perturbation. The term with coefficient Γ_0 in the pressure equation represents the effect due to plasma compressibility. The term $\vec{\nabla}\cdot\vec{\tilde{V}}_\perp \sim -\tilde{V}_\perp\cdot(\vec{\nabla}\ln B + \vec{\kappa})$ describes the perpendicular part of the plasma compressibility.

With perturbations of the form $f(\vec{x},t)=f(x)\exp[i(k_y y - \omega t)], \nabla_\parallel = ik_\parallel(x) = ik_y x/L_s$, the normalized eigenvalue equation becomes

$$\frac{d}{dX}\left[(\hat{\omega}^2 - X^2)\frac{d\phi}{dX}\right] - \left[\hat{\omega}^2 - X^2 + D_I \times\left\{1 - 2\Gamma_0\frac{r_p}{R_c}\frac{\hat{\omega}^2}{\left(\hat{\omega}^2 - \frac{\Gamma_0}{2}\beta X^2\right)}\right\}\right]\phi = 0. \quad (7)$$

Here, we have defined a normalized distance $X \equiv k_y x$ and frequency $\hat{\omega} \equiv \omega/(V_A/L_s)$, $D_I \equiv \beta L_s^2/(R_c r_p)$, $r_p = |d\ln P_0/dx|^{-1}$ is the equilibrium density gradient scale length, and $\beta \equiv 8\pi P_0/B^2 \equiv C_s^2/V_A^2$. The terms with coefficient $\hat{\omega}^2$ arise from the divergence of the polarization current, the terms proportional to X^2 represent the magnetic field line bending physics brought about by magnetic shear and D_I is the combination of the pressure gradient and curvature effects which represents the source of free energy. The term with coefficient Γ_0 represents the sound wave coupling effect and is important when $\hat{\omega}^2 \sim \beta X^2$.

III. EIGENVALUE ANALYSIS

We now solve the eigenvalue equation analytically using a matched asymptotic analysis method.[18] Here, the equation is divided into three regions: (1) inner region where the inertial effects dominate; (2) intermediate region where the compressible effects, i.e., sound effects, plays a dominant role; and (3) outer region, i.e., large X region, similar to the one used in Ref. 19. This matching procedure is valid for $|\hat{\omega}^2| \ll 1$ and $\Gamma_0\beta \ll 1$. Since the equation is symmetric in X, it is sufficient to solve this equation only for $X \geq 0$.

In the inner region, i.e., $|X^2| \sim |\hat{\omega}^2|$, for $\Gamma_0\beta \ll 1$ with $Z = X^2/\hat{\omega}^2$ and $\hat{\omega}^2 \ll 1$, Eq. (7) reduces to

$$Z(1-Z)\frac{d^2\phi}{dZ^2} + \left(\frac{1}{2} - \frac{3}{2}Z\right)\frac{d\phi}{dZ} - \frac{D_I}{4}\left(1 - 2\Gamma_0\frac{r_p}{R_c}\right)\phi = 0, \quad (8)$$

which is a hypergeometric equation[21] whose general solution is

$$\phi_I = A_I F\left(\frac{1}{4} + \frac{p}{2}, \frac{1}{4} - \frac{p}{2}; \frac{1}{2}; \frac{X^2}{\hat{\omega}^2}\right) + B_I\sqrt{\frac{X^2}{\hat{\omega}^2}}F\left(\frac{3}{4} + \frac{p}{2}, \frac{3}{4} - \frac{p}{2}; \frac{3}{2}; \frac{X^2}{\hat{\omega}^2}\right), \quad (9)$$

with

$$p = \sqrt{\frac{1}{4} - D_I\left(1 - 2\Gamma_0\frac{r_p}{R_c}\right)}.$$

The choice of the coefficients A_I, B_I depends on the parity condition at $X=0$. For even modes, the boundary condition at $X=0$ is $d\phi/dX=0$, which demands that $B_I=0$. For odd modes, the boundary condition at $X=0$ is $\phi=0$, which ensures that $A_I=0$. Here, we consider only the even mode solution because it is the most unstable mode.

In the intermediate region, where sound effects become important, $\Gamma_0\beta X^2 \sim \hat{\omega}^2$, Eq. (7) with $Z=\Gamma_0\beta X^2/2\hat{\omega}^2$ becomes

$$Z^2\frac{d^2\phi}{dZ^2} + \frac{3}{2}Z\frac{d\phi}{dZ} + \left[\frac{D_I}{4} - \frac{\Gamma_0}{2}\frac{r_p}{R_c}\frac{D_I}{(1-Z)}\right]\phi = 0. \quad (10)$$

With $\phi=(-Z)^{-1/4+p/2}F(Z)$, the function $F(Z)$ satisfies a hypergeometric equation and the general solution for ϕ in the intermediate region is given by

$$\phi_{II} = \left(-\frac{\Gamma_0}{2}\frac{\beta X^2}{\hat{\omega}^2}\right)^{-1/4+p/2}\left[A_{II}F\left(a,b;c;\frac{\Gamma_0}{2}\frac{\beta X^2}{\hat{\omega}^2}\right) + B_{II}\left(\frac{\Gamma_0}{2}\frac{\beta X^2}{\hat{\omega}^2}\right)^{1-c}F\left(-b,-a;2-c;\frac{\Gamma_0}{2}\frac{\beta X^2}{\hat{\omega}^2}\right)\right], \quad (11)$$

where $a=(p+i\lambda)/2$, $b=(p-i\lambda)/2$, $c=1+p$ and $\lambda = \sqrt{D_I - 1/4}$.

Finally, in the outer region (i.e., $|X^2| \gg |\hat{\omega}^2|$), Eq. (7) becomes

$$\frac{d}{dX}\left(X^2\frac{d\phi}{dX}\right) + (D_I - X^2)\phi = 0. \quad (12)$$

In the limit $D_I \gg X^2$, this equation is the same as that analyzed by Suydam[1,2] from which he obtained the stability criterion $D_I \leq 1/4$. With $Z=2X$ and $\phi=\hat{\phi}/Z$, Eq. (12) becomes a Whittaker equation.[20,21] The Whittaker function solution for a growing mode, which decays as $X\to\infty$, is given by

$$\phi_o = A_{III}\frac{\exp(-X)}{\sqrt{2X}}(2X)^{i\lambda}U\left(\frac{1}{2} + i\lambda, 1 + 2i\lambda, 2X\right), \quad (13)$$

where U is Kummer's confluent hypergeometric function.

Next, we match the inner (ϕ_I) and intermediate (ϕ_{II}) solutions in their overlap region. For the outer limit of the inner region solution (i.e., when $|X|\to\infty$), we obtain

$$\phi_I^o \sim \frac{A_I\sqrt{\pi}\Gamma(p)}{\left[\Gamma\left(\frac{1}{4}+\frac{p}{2}\right)\right]^2}\left(-\frac{X^2}{\hat{\omega}^2}\right)^{-1/4+p/2} \times\left[1+\frac{\Gamma(-p)}{\Gamma(p)}\left\{\frac{\Gamma\left(\frac{1}{4}+\frac{p}{2}\right)}{\Gamma\left(\frac{1}{4}-\frac{p}{2}\right)}\right\}^2\left(-\frac{X^2}{\hat{\omega}^2}\right)^{-p}\right].$$

For the inner limit of the intermediate region solution (i.e., when $|X|\to 0$), we obtain

$$\phi_{II}^i \sim \left(-\frac{\Gamma_0\beta X^2}{2\hat{\omega}^2}\right)^{-1/4+p/2} A_{II}\left[1+\frac{B_{II}}{A_{II}}\left(\frac{\Gamma_0\beta X^2}{2\hat{\omega}^2}\right)^{-p}\right].$$

On comparing ϕ_I^o with ϕ_{II}^i, we obtain

$$A_{II}=\frac{A_I\sqrt{\pi}\Gamma(p)}{\left[\Gamma\left(\frac{1}{4}+\frac{p}{2}\right)\right]^2}\left(\frac{2}{\Gamma_0\beta}\right)^{-1/4+p/2} \tag{14}$$

and

$$\frac{B_{II}}{A_{II}}=\frac{\Gamma(-p)}{\Gamma(p)}\left\{\frac{\Gamma\left(\frac{1}{4}+\frac{p}{2}\right)}{\Gamma\left(\frac{1}{4}-\frac{p}{2}\right)}\right\}^2\left(-\frac{2}{\Gamma_0\beta}\right)^{-p}. \tag{15}$$

We next match the intermediate region solution to the outer solution in their overlapping region. The outer limit of the intermediate region solution with coefficients A_{II} and B_{II} [given by Eqs. (14) and (15)] is

$$\phi_{II}^o \sim \frac{A_I\sqrt{\pi}\Gamma(p)\Gamma(i\lambda)}{\left[\Gamma\left(\frac{1}{4}+\frac{p}{2}\right)\right]^2}\left(-\frac{X^2}{2\hat{\omega}^2}\right)^{-1/4+i(\lambda/2)} \times C_1^\infty\left[1+\frac{\Gamma(-i\lambda)}{\Gamma(i\lambda)}\frac{C_2^\infty}{C_1^\infty}\left(-\frac{\hat{\omega}^2}{X^2}\right)^{i\lambda}\right],$$

where

$$C_1^\infty=\frac{\Gamma(1+p)}{\Gamma(a)\Gamma(1+a)}\left(\frac{\Gamma_0\beta}{2}\right)^{-b} +\frac{\Gamma(-p)\Gamma(1-p)}{\Gamma(p)\Gamma(-b)\Gamma(1-b)}\left\{\frac{\Gamma\left(\frac{1}{4}+\frac{p}{2}\right)}{\Gamma\left(\frac{1}{4}-\frac{p}{2}\right)}\right\}^2\left(\frac{\Gamma_0\beta}{2}\right)^{a} \tag{16}$$

and

$$C_2^\infty=\frac{\Gamma(1+p)}{\Gamma(b)\Gamma(1+b)}\left(\frac{\Gamma_0\beta}{2}\right)^{-a} +\frac{\Gamma(-p)\Gamma(1-p)}{\Gamma(p)\Gamma(-a)\Gamma(1-a)}\left\{\frac{\Gamma\left(\frac{1}{4}+\frac{p}{2}\right)}{\Gamma\left(\frac{1}{4}-\frac{p}{2}\right)}\right\}^2\left(\frac{\Gamma_0\beta}{2}\right)^{b}. \tag{17}$$

Finally, the inner limit of the outer solution ϕ_{III} is

$$\phi_{III}^i \sim A_{III}\sqrt{\frac{\pi}{2X}}\left(\frac{1}{2\lambda\Gamma(i\lambda)\sinh\lambda\pi}\right) \times\left[1+\frac{\Gamma(i\lambda)}{\Gamma(-i\lambda)}\left(\frac{2}{X}\right)^{2i\lambda}\right]\left(\frac{X}{2}\right)^{i\lambda}.$$

On comparing the outer limit of the intermediate region solution with the inner limit of outer solution, we obtain the eigenvalue equation

$$\left(-\frac{\hat{\omega}^2}{4}\right)^{i\lambda/2}=\exp(-i\pi)\frac{\Gamma(1+i\lambda)}{\Gamma(1-i\lambda)}\sqrt{\frac{C_1^\infty}{C_2^\infty}}, \tag{18}$$

where C_1^∞ and C_2^∞ are given by Eqs. (16) and (17), respectively. In the following subsections, we examine two cases related to the amplitude of D_I relative to $(1/4)(1-\Gamma_0 r_p/2R_c)^{-1}$.

A. $p^2 \geqslant 0$ case

This corresponds to the case when Suydam's criterion is weakly violated. For $D_I \leqslant (1/4)(1-\Gamma_0 r_p/2R_c)^{-1}$, the value of the parameter $p=\pm\sqrt{1/4-D_I(1-2\Gamma_0 r_p/R_c)}$ is real. The coefficient C_1^∞ is the complex conjugate of C_2^∞. Thus, the normalized growth rate $(-\hat{\omega}^2\equiv\hat{\gamma}^2)$ of the mode is given by

$$\hat{\gamma}=2\exp\left(-\frac{(\pi-2\Theta_1-\Theta_2)}{|\lambda|}\right), \tag{19}$$

where Θ_1 is the phase of the Gamma function $\Gamma(1+i\lambda)$ and Θ_2 is the phase of the coefficient C_1^∞, both depending on $\lambda=\sqrt{D_I-1/4}$. As $|\lambda|\to 0$, coefficients C_1^∞ and C_2^∞ become real and the asymptotic limits $\Theta_1\to 0$ and $\Theta_2\to 0$ are obtained. Thus, the above expression clearly indicates that marginal stability can be approached from the unstable region when $D_I\to 1/4(|\lambda|\to 0)$. The normalized growth for $D_I\geqslant 1/4$ is $\hat{\gamma}\approx\exp(-\pi/|\lambda|)\to 0$. Thus, the marginal stability condition in the compressible case is the same as the Suydam criterion in an incompressible plasma.

B. $p^2<0$ case

This case corresponds to a strong violation of the Suydam criterion. Here, the parameter $p=i\lambda_0$ is purely imaginary and $\lambda_0=\pm\sqrt{D_I(1-2\Gamma_0 r_p/R_c)-(1/4)}$. In this limit, the coefficient C_2^∞ is given as

$$C_2^\infty=\frac{\Gamma(-i\lambda_0)}{\Gamma(i\lambda_0)}\left\{\frac{\Gamma\left(\frac{1}{4}+i\frac{\lambda_0}{2}\right)}{\Gamma\left(\frac{1}{4}-i\frac{\lambda_0}{2}\right)}\right\}^2(C_1^\infty)^*.$$

Thus, the dispersion relation can be written as

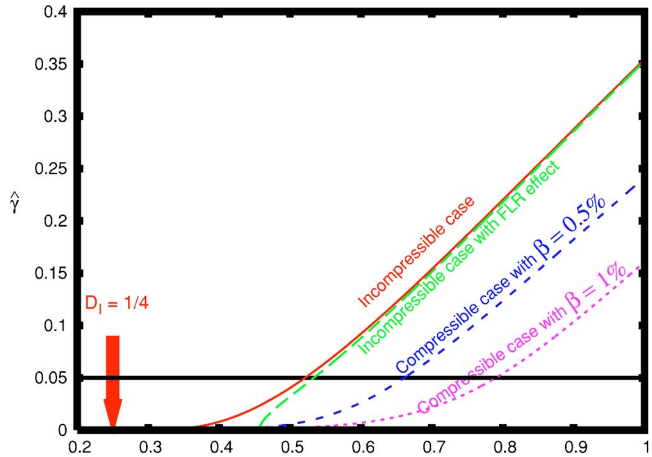

FIG. 1. Normalized growth rate $\hat{\gamma}$ versus D_I shows the stabilizing effect of compressibility.

$$\left(-\frac{\hat{\omega}^2}{4}\right)^{i\lambda/2} = \exp(-i\pi)\frac{\Gamma(1+i\lambda)}{\Gamma(1-i\lambda)}\frac{\Gamma\left(\frac{1}{4}-i\frac{\lambda_0}{2}\right)}{\Gamma\left(\frac{1}{4}+i\frac{\lambda_0}{2}\right)}\left\{\frac{\Gamma(i\lambda_0)}{\Gamma(-i\lambda_0)}\frac{C_1^\infty}{(C_1^\infty)^*}\right\}^{1/2}. \tag{20}$$

This gives a purely growing mode with normalized growth rate $(\hat{\gamma}^2 \equiv -\hat{\omega}^2)$

$$\hat{\gamma} = 2\exp\left[-\frac{1}{|\lambda|}(\pi - 2\Theta_1 - \Theta_2 - 2\Theta_3 - \Theta_4)\right], \tag{21}$$

where Θ_1 is the phase of the Gamma function $\Gamma(1+i\lambda)$, Θ_2 is the phase of the coefficient C_1^∞, Θ_3 is the phase of the Gamma function $\Gamma(1/4-i\lambda_0/2)$ and Θ_4 is the phase of the Gamma function $\Gamma(i\lambda_0)$. All are functions of λ and λ_0.

The growth rate in the case of an incompressible ideal interchange instability can be easily derived from the above equation. With $\Gamma_0\beta \ll 1$, the parameter $\lambda_0 \to \lambda$. Hence, the coefficient $C_1^\infty \to 1/\Gamma(i\lambda)$ and the dispersion relation is given as

$$\left(-\frac{\hat{\omega}_{inc}^2}{4}\right)^{i\lambda/2} = \exp(-i\pi)\frac{\Gamma(1+i\lambda)}{\Gamma(1-i\lambda)}\frac{\Gamma\left(\frac{1}{4}-i\frac{\lambda}{2}\right)}{\Gamma\left(\frac{1}{4}+i\frac{\lambda}{2}\right)}, \tag{22}$$

which yields the normalized growth rate $(\hat{\gamma}_{inc} = -\hat{\omega}_{inc}^2)$

$$\hat{\gamma}_{inc} = 2\exp\left[-\frac{(\pi - 2\Theta_1 - 2\Theta_5)}{|\lambda|}\right], \tag{23}$$

where Θ_5 is the phase of the Gamma function $\Gamma(1/4 - i\lambda/2)$.

Finally, we solve the full dispersion relation Eq. (18) numerically for different values of D_I, with $\beta = 0.5\%$ and $\beta = 1\%$. The normalized growth rates of an ideal interchange instability for both the incompressible and compressible cases are shown in Fig. 1. The figure clearly indicates that compressibility has a stabilizing effect on the interchange instability. It also indicates that near $D_I = 1/4$ the growth rate is similar to the one obtained in the incompressible case. The reduction factor for normalized growth rate induced by compressibility can also be determined from Eqs. (19) and (23) or Eqs. (21) and (23); and it depends on the value of β. We have also shown the effects of finite Larmor radius (FLR) on the incompressible case, as shown in Ref. 12. The solid line at $\hat{\gamma} \sim 0.05$ for all values of D_I represents the normalized growth rate below which FLR effects have a stabilizing effect on the incompressible ideal interchange instability. Similar stabilizing effects, due to a ion FLR, should also be observed for the compressible interchange instability. In the case of the compressible interchange instability, the value of $\hat{\gamma} \sim 0.05$ below which FLR effects have a stabilizing effect, corresponds to $D_I \gtrsim 0.75$ for $\beta \sim 1\%$. Thus, in the presence of compressibility and FLR effects, the criterion for robust growth rate is about a factor of 3 larger than the Suydam's criterion $D_I > 1/4$, however, the precise criterion depends upon β.

IV. CONCLUSION

In this paper, we have investigated the effects of plasma compressibility on the linear eigenmode and growth rate for a magnetic-shear-localized ideal interchange instability in a simple sheared slab geometry, which represents the key magnetic shear and curvature effects of axisymmetric (e.g., tokamak) and nonaxisymmetric (e.g., stellarators) toroidal geometries. A linear eigenvalue equation was derived and solved using a matched asymptotic analysis. The equation was solved in three subregions: (1) inner region where inertial effects are dominant, (2) intermediate region, where the sound effects are dominant, and (3) large $|X|$ region where the dynamics is governed by the pressure drive and field line bending terms. A marginal stability condition at $D_I = 1/4$ is found to be consistent with the conventional Suydam analysis. The simple sheared slab model and our analysis is easily generalizable to different types of toroidal devices. Thus, the results obtained from this analysis are applicable to both tokamaks and stellarators. The effect of compressibility does not alter the marginal stability condition. However, when the instability boundary is crossed, compressibility reduces the magnitude of the growth rate of ideal MHD interchange instability.

ACKNOWLEDGMENTS

This work was supported by the U.S. Department of Energy under Grant No. DE-FG02-86ER53218.

[1] J. P. Friedberg, *Ideal Magnetohydrodynamics* (Plenum, New York, 1987), Chaps. 9 and 10.
[2] B. R. Suydam, in *Second United Nations International Conference on the Peaceful Uses of Atomic Energy* (United Nations, Geneva, 1958), Vol. 31, p. 157.
[3] C. Mercier, Nucl. Fusion **1**, 47 (1960).
[4] V. D. Shafranov and E. I. Yurchenko, Sov. Phys. JETP **26**, 682 (1968).
[5] N. Yanagi, S. Morimoto, K. Ichiguchi, S. Besshou, M. Sato, S. Kobayashi, M. Iima, H. Nakamura, M. Wakatani, and T. Obiki, Nucl. Fusion **32**, 1264 (1992).
[6] S. Okamura *et al.*, in *Proceedings of the 15th International Conference on*

Plasma Physics and Controlled Nuclear Fusion Research (International Atomic Energy Agency, Vienna, 1995), Vol. 1, p. 381.
[7] S. Okamura, K. Matsuoka, R. Akiyama *et al.*, Nucl. Fusion **39**, 1337 (1999).
[8] K. Y. Watanabe, A. Weller, S. Sakakibara *et al.*, Fusion Sci. Technol. **46**, 24 (2004).
[9] K. Y. Watanabe *et al.*, J. Plasma Fusion Res. (to be published).
[10] R. M. Kulsrud, Phys. Fluids **6**, 904 (1963).
[11] T. E. Stringer, Nucl. Fusion **15**, 125 (1975).
[12] S. Gupta, J. D. Callen, and C. C. Hegna, Phys. Plasmas **9**, 3395 (2002).
[13] H. P. Furth, J. Killeen, and M. N. Rosenbluth, Phys. Fluids **6**, 459 (1963).
[14] B. Coppi, Phys. Rev. Lett. **12**, 417 (1964).
[15] B. Coppi, J. M. Greene, and J. L. Johnson, Nucl. Fusion **6**, 101 (1966).
[16] S. E. Kruger, C. C. Hegna, and J. D. Callen, Phys. Plasmas **5**, 4169 (1998).
[17] R. D. Hazeltine and J. D. Meiss, *Plasma Confinement* (Addison-Wesley, Redwood City, CA, 1992), Chap. 7, p. 258.
[18] C. M. Bender and S. A. Orszag, *Advanced Mathematical Methods for Scientists and Engineers* (McGraw-Hill, New York, 1978), Chap. 9, p. 419.
[19] A. B. Mikhailvoskii and A. A. Skovoroda, Plasma Phys. Controlled Fusion **44**, 2033 (2002).
[20] M. Abramowitz and I. A. Stegun, *Handbook of Mathematical Functions* (Dover, New York, 1964), Chap. 9.
[21] W. Magnus, F. Oberhettinger, and R. P. Soni, *Formulas and Theorems for the Special Functions of Mathematical Physics* (Springer-Verlag, Berlin, 1966), Chap. II.